Intrinsic anomalous magnetic anisotropy of CdCr$_2$S$_4$

D. Ehlers, V. Tsurkan, H.-A. Krug von Nidda, and A. Loidl

Experimental Physics V, Centre for Electronic Correlations and Magnetism, University of Augsburg, 86135 Augsburg, Germany

The magnetocrystalline anisotropy of the ferromagnetic spinel CdCr$_2$S$_4$ was investigated by ferromagnetic resonance measurements. By avoiding any contact to iron during the sample preparation we can exclude that the anisotropy is due to ferrous impurities, and by performing wavelength dispersive electron probe microanalysis as well as annealing experiments, it is demonstrated that the samples possess almost ideal stoichiometry. The resonance data suggest that compositional deviations from the stoichiometry up to 10^{-3} have no influence on our conclusion that the magnetocrystalline anisotropy is an intrinsic property of CdCr$_2$S$_4$, caused by trigonal distortion of the sulfur octahedra surrounding the Cr^{3+} ions. Anomalous low-temperature linewidth maxima in the $\langle 111 \rangle$ directions can be understood by considering the crystal fields acting on inequivalent sites of the magnetic ions in the spinel structure and by taking into account the effect of exchange narrowing.

I. INTRODUCTION

The magnetic chromium spinels ACr$_2X_4$ (A = Cd, Mg, Zn, and Hg; X = O, S, and Se) represent a class of compounds allowing one to analyze in detail the interplay of lattice, charge, orbital, and spin degrees of freedom and to systematically study the competition of antiferromagnetic and ferromagnetic direct exchange and superexchange interactions dependent on the size of anions and cations.[1–3] Concerning the magnetic order, the pyrochlore lattice of the chromium ions may give rise to strongly geometrically frustrated antiferromagnetism which is particularly observed in many chromium oxide spinels,[1,4] where direct Cr^{3+}-Cr^{3+} exchange governs the magnetism due to the short distance between the magnetic ions. As the lattice constant increases with increasing ionic radii, however, superexchange also comes into play and bond frustrated magnetism can be observed, like in some of the thiospinels. In the magnetic semiconductor CdCr$_2$S$_4$ the exchange is dominated by the 90° Cr^{3+}-S^{2-}-Cr^{3+} superexchange path, leading to a ferromagnetically ordered ground state.[5] The ferromagnetic Curie temperature $T_C = 84.5$ K and a saturated moment $M_s \cong 3\mu_B$/Cr^{3+} agree well with the expectation for the electronic configuration [Ar] $3d^3$, where the spin value is $S = \frac{3}{2}$ and the orbital moment for the t_{2g}^3 ground state is quenched.

Multiferroic behavior in this material[6] as well as in HgCr$_2$S$_4$ and CdCr$_2$Se$_4$ (Refs. 7 and 8) has attracted considerable interest, while the origin of the relaxor ferroelectric properties still has not been clarified. Yet, the strong magnetocapacitive coupling below $T \approx 150$ K allows the conclusion that the magnetic Cr^{3+} ions must play a crucial role in the ferroelectric ordering mechanism. Other remarkable properties of CdCr$_2$S$_4$ have been observed, such as a strong blueshift of the optical absorption edge below $T \approx 150$ K,[9] coinciding with a softening of the lattice.[10] The results may point to structural changes that cause the multiferroic phase. Furthermore, at low temperatures $T < 20$ K, the dielectric constant drops drastically.[6] Interestingly, this is accompanied by an excess contribution to the specific heat[11] and the emergence of a pronounced magnetocrystalline anisotropy in the same temperature range.

There has been a controversial discussion whether the observed magnetocrystalline anisotropy of this material (first

anisotropy constant $K_1 \approx 4 \times 10^4 \frac{\text{erg}}{\text{cm}^3}$ at $T = 4$ K) is of intrinsic nature. Berger and Pinch observed anisotropies differing from sample to sample,[12] which they attributed to deviations from ideal stoichiometry,[13] in particular, to the presence of Cr^{2+} ions on octahedral spinel sites. While the Jahn-Teller active Cr^{2+} ion would yield a tetragonal distortion and a corresponding crystal field, Cr^{3+} is not Jahn-Teller active and a cubic crystal field is not sufficient to lift the fourfold degeneracy of the spin states in Cr^{3+}.[14] Hoekstra *et al.* later stated that the anisotropy has rather to be explained by Fe^{3+} impurities on the spinel's tetrahedral sites.[15,16] Nevertheless, the detailed angular dependence of the ferromagnetic resonance (FMR) fields and of the corresponding linewidths has left open questions.[12,17] The aim of this work is to present our recent FMR results on CdCr$_2$S$_4$ samples without the above-mentioned defects and, based on them, to elucidate the subjects concerning the origin of the observed FMR anisotropy.

II. EXPERIMENTAL DETAILS

The single crystals were grown by chemical transport reactions using the preliminarily synthesized polycrystalline ternary compound. The polycrystalline material was prepared from high-purity starting materials (CdS, 99.99%; Cr, 99.99%; and S, 99.999%). The starting materials taken in stoichiometric ratio were pressed into pellets using a titanium press in order to avoid any contact with iron during the sample preparation. For the single-crystal growth, TeBr$_4$ (99.999%) served as a transport agent. The polycrystalline material and the transport agent were inserted in a quartz ampoule which was evacuated to 10^{-3} mbar and closed. The growth process was performed between 850 and 900 °C during three to four weeks. The grown crystals have the shape of octahedra with a dimension up to 3 mm on edge with a shiny gray surface. We have demonstrated that using bromine as the transport agent allows one to improve the crystals' purity compared to earlier used chlorine which contaminates the crystals due to substitution of sulfur.[18] Sharp diffraction lines and the absence of any foreign phase peaks in the x-ray diffraction patterns of the starting polycrystalline materials as well as of the crashed single crystals obtained on

a Bragg-Brentano transmission setup (STOE STADI P with a linear position sensitive detector) confirmed the high purity of the samples. Furthermore, wavelength dispersive electron probe microanalysis of the single crystals using a Camebax SX 50 spectrometer did not find any impurity contamination by the suspected elements Fe, Te, and Br. The detection limit of the spectrometer was estimated[19] to be less than 2×10^{-4} for Fe and 1×10^{-3} for Te and Br. The composition of the untreated sample was determined by averaging over ten points and found to be stoichiometric within the accuracies 1 mol % for Cd, 0.5 mol % for Cr, and 1.5 mol % for S. Raman-scattering spectra of these samples[20] reveal a low background and the well-defined excitations with narrow line shapes allow the same conclusion of perfectly grown crystals. For the purpose of FMR measurements these were shaped into thin disks in a (110) plane and polished to optical quality by a $0.25 \mu m$ diamond paste.

For studies of disorder effects and of the consequences due to deviations from stoichiometry, one sample was annealed in vacuum for 72 h at 750 °C. During this reaction, it is expected that sulfur diffuses towards the surface and Cr^{3+} is reduced to Cr^{2+}. Another sample of $CdCr_2S_4$ was annealed for seven days in an oxidizing sulfur atmosphere at 750 °C and at a sulfur pressure of 7 bars. It was intended to remove possible residual Cr^{2+} by this treatment.

The FMR studies were performed with a continuous-wave X-band spectrometer (Bruker ELEXSYS E500). For cooling in the temperature range $4\,K < T < 300\,K$, a continuous He gas-flow cryostat (Oxford Instruments) was used and the temperature stability was $\sim 0.2\,K$. The magnetic field was applied in the (110) disk plane and, using a goniometer with an accuracy of $< 1°$, the samples could be rotated with the axis of rotation perpendicular to the disk plane. The microwave frequency was $\nu = 9.36\,GHz$ for all performed measurements and the applied field H could be swept up to 18 kOe. Due to the use of lock-in technique, the absorption signal is the first derivative of a Lorentzian. Supplementary magnetization measurements were obtained on a Quantum Design MPMPS XL SQUID magnetometer.

III. FMR RESULTS

Figure 1 presents the FMR spectra at the lowest available temperature with the field applied along the three main crystallographic directions of the cubic structure—$\langle 100 \rangle$, $\langle 111 \rangle$, and $\langle 110 \rangle$—which are all found in the (110) plane. In addition to the main resonances, one observes several satellite resonances, smaller in amplitude, which are ascribed to the excitation of magnetostatic modes of higher order.[21] For our considerations on the anisotropy we concentrate on the main line corresponding to the uniform precession mode of the magnetization. Resonance fields and linewidths are obtained from a fit by the first derivative of a Lorentzian line which is only slightly asymmetric due to a small contribution of dispersion in the absorption spectra. It is evident that both resonance field and linewidth are considerably anisotropic. The detailed observed anisotropy within the (110) plane is plotted in Fig. 2 (dots). Due to the symmetry, the range between 0° and 90° essentially contains all information. We ascribe small deviations to a nonperfect orientation of the
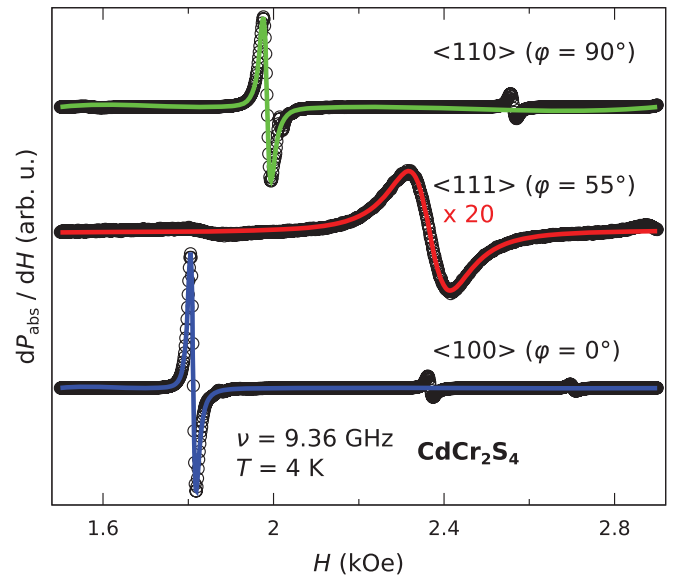

FIG. 1. (Color online) FMR spectra for a $CdCr_2S_4$ single crystal at $T = 4$ K with the static magnetic field H applied along the principal cubic axes.

single crystal. The picture of the resonance field's angular dependence with minima at 0° and 90° and a maximum at 55° (corresponding to the directions $\langle 100 \rangle$, $\langle 110 \rangle$, and $\langle 111 \rangle$, respectively) qualitatively suggests a positive cubic anisotropy, as has already been reported by Berger and Pinch,[12,13] with the low minimum corresponding to the easy direction of magnetization and the maximum to the hard one. Huge
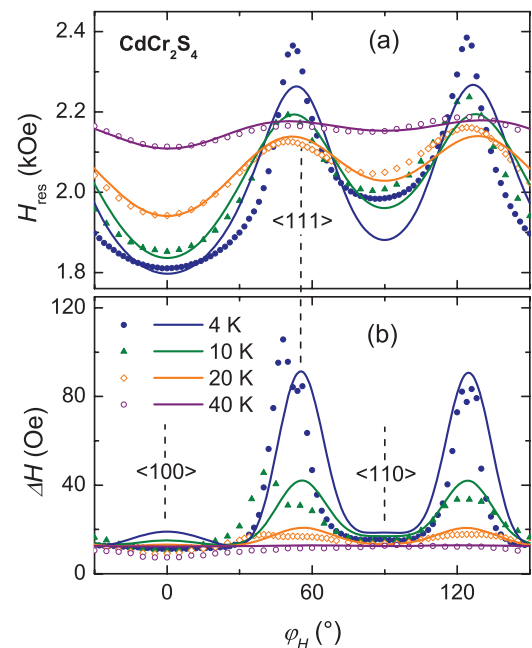

FIG. 2. (Color online) Angular dependencies of the resonance field (a) and of the FMR linewidth (b) in as-grown $CdCr_2S_4$. The experimental data are shown by the dots at four temperatures. The angle φ_H is defined as the angle between magnetic field and the [100] direction. The lines indicate fits for the range from 0° to 90° by the described uniaxial model.
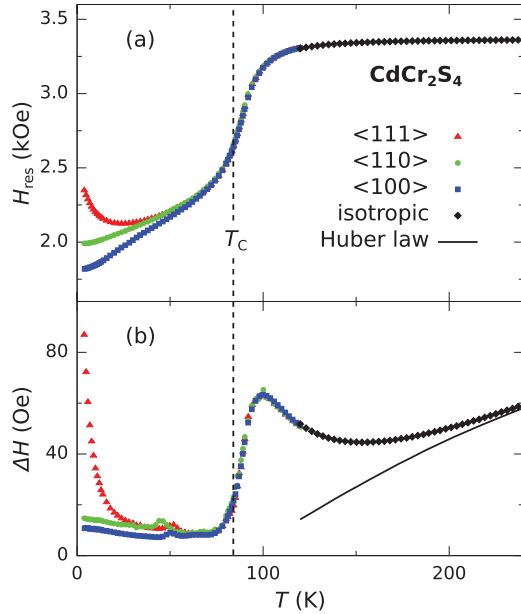
FIG. 3. (Color online) Temperature dependence of the resonance field (a) and of the FMR linewidth (b) in as-grown CdCr$_2$S$_4$ for the crystallographic main directions. At high temperatures the signal is isotropic and the solid line is from a Huber law approximation to the high-temperature linewidth data.

FIG. 4. (Color online) Temperature dependencies of the resonance field (a) and of the FMR linewidth (b) in vacuum annealed CdCr$_2$S$_4$. The inset shows the corresponding angular dependencies at 20 and 40 K. For comparison, the resonance field anisotropy of the as-grown CdCr$_2$S$_4$ crystal at 4 K is replotted in the upper frame. The line gives the fit of cubic anisotropy.

anisotropy also is observed in the angular dependence of the linewidth [Fig. 2(b)]. Along the $\langle 111 \rangle$ direction a maximum up to $\Delta H \approx 100$ Oe at 4 K with a width of around $\pm 15°$ occurs, whereas in the other directions the residual value of the linewidth amounts to ~ 10 Oe, a value that can be well explained by the relaxation due to surface pits.[22] The maximum coincides with that direction where the resonance field also shows its maximum. Temperature-dependent results in the three main directions are plotted in Fig. 3. First of all, with decreasing temperature one notes a drop of H_{res} at T_C, which is due to the demagnetizing effect for our sample geometry. The magnetocrystalline anisotropy appears below 60 K and $H_{\text{res}}^{\langle 111 \rangle} - H_{\text{res}}^{\langle 100 \rangle}$ reaches 550 Oe at 4 K. In the high-temperature limit, H_{res} saturates and it provides the g-factor value of 1.985 ± 0.002, which means weak spin-orbit coupling as expected for the half-filled t_{2g}^3 state. The strong drop of ΔH at T_C is explained by the vanishing random dipolar field distribution in the ferromagnetic phase. The above-mentioned linewidth maximum in $\langle 111 \rangle$ evolves below 25 K and small and slightly anisotropic linewidth maxima are observed at ~ 50 K. Approaching the ferromagnetic transition from the isotropic paramagnetic side, the increase of the linewidth is well described as a critical speeding-up of the spin-relaxation rate, which arises from increasing lifetime and correlation length of magnetization fluctuations.[23–25] On the other hand, the increase of ΔH towards high temperatures above 150 K may be explained[26] as resulting from the law $\Delta H T I_{\text{ESR}} = \text{const.}$, pointed out by Huber.[27] In between, a minimum of the linewidth is observed in the paramagnetic region at $T \approx 150$ K.

The FMR results obtained from the vacuum annealed (VA) sample are depicted in Fig. 4, where one recognizes that the magnetocrystalline anisotropy has drastically increased, as
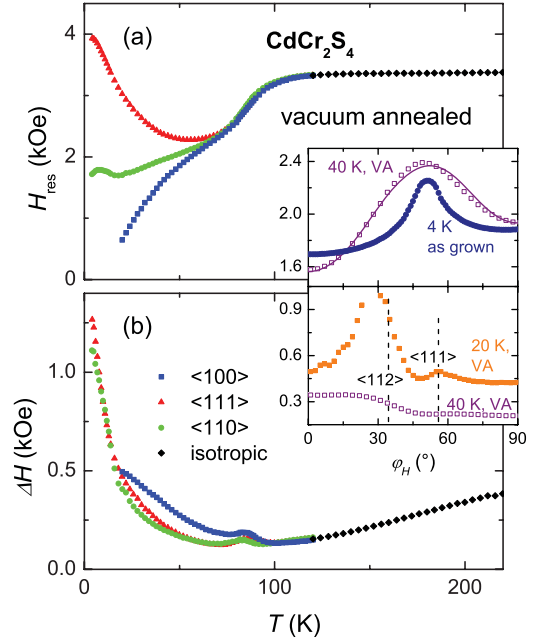
$H_{\text{res}}^{\langle 111 \rangle} - H_{\text{res}}^{\langle 100 \rangle} = 800$ Oe even at 40 K, which is considerably higher than for the untreated sample at 4 K. Although the anomalies along the $\langle 112 \rangle$ and $\langle 110 \rangle$ directions (the huge maximum at $\varphi \approx 30°$ seems to be due to evaluation difficulties) expected for Cr^{2+} (Ref. 16) cannot clearly be identified, we conclude that Cr^{2+} on octahedral sites produces a much higher anisotropy than Cr^{3+}, in agreement with the earlier observations.[13] It has to be noted that the temperature dependence of ΔH, in principal, behaves similarly compared to the untreated sample, although the FMR lines now are substantially broader. For the sample annealed in sulfur atmosphere (SA), the magnitude of the anisotropy is only slightly smaller after the treatment, with $H_{\text{res}}^{\langle 111 \rangle} - H_{\text{res}}^{\langle 100 \rangle} = 480$ Oe at $T = 4$ K (see Fig. 5). Again, an anomaly in ΔH remains visible above an isotropic residual contribution, which is, as for VA, considerably higher compared to the "as-grown" samples.

IV. ANALYSIS AND DISCUSSION

The Cr^{3+} ions are located on the octahedral sites of the spinel lattice and are surrounded by six nearest S^{2-} neighbors, which primarily cause a cubic crystal field on the Cr^{3+} ions. As a consequence, their orbital ground state becomes a ^4A singlet. Due to the anions' finite size, the CrS$_6$ octahedra are trigonally distorted along the cubic space diagonals. This leads to an additional trigonal crystal-field contribution, resulting in a zero-field splitting of the four spin states of the Cr^{3+} ions into two Kramers doublets.[14] As there exist four distinct octahedral sites in the spinel lattice with trigonal axis each along one of the cubic space diagonals [111], [$\bar{1}$11], [1$\bar{1}$1], and [11$\bar{1}$], effectively,
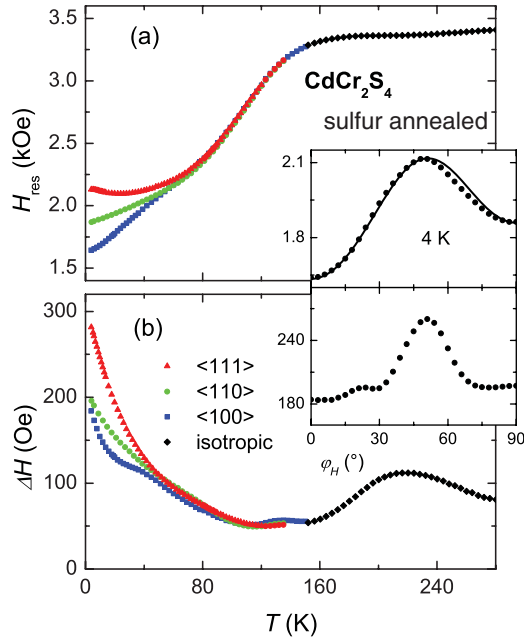
FIG. 5. (Color online) Temperature dependencies of the resonance field (a) and of the FMR linewidth (b) in sulfur annealed $CdCr_2S_4$. The inset shows the corresponding angular dependencies at 4 K. The line reflects the fit of cubic anisotropy.

cubic magnetocrystalline anisotropy is expected to be observed as a superposition of the four sites' anisotropic FMR signals.

Cubic anisotropy is described by the magnetocrystalline free anisotropy energy density in the form

$$F_{an} = K_1^c\left(\alpha_1^2\alpha_2^2 + \alpha_1^2\alpha_3^2 + \alpha_2^2\alpha_3^2\right) + K_2^c\left(\alpha_1^2\alpha_2^2\alpha_3^2\right)$$
$$+ K_3^c\left(\alpha_1^2\alpha_2^2 + \alpha_1^2\alpha_3^2 + \alpha_2^2\alpha_3^2\right)^2 + \cdots, \quad (1)$$

where K_n^c denotes the cubic anisotropy constants of nth order and the α_j are the direction cosines of the magnetization with respect to the cubic axes [100], [010], and [001]. The resonance condition is given by the Smit-Suhl formula[28]

$$\frac{\omega_0}{\gamma} = \frac{1}{M_0\sin\theta_0}\left[\frac{\partial^2 F}{\partial\theta^2}\frac{\partial^2 F}{\partial\varphi^2} - \left(\frac{\partial^2 F}{\partial\theta\partial\varphi}\right)^2\right]^{1/2}, \quad (2)$$

where ω_0 is the radiation angular frequency, γ is the spectroscopic ratio of Cr^{3+}, and F contains all anisotropic magnetic energy contributions. θ and φ denote the polar and azimuthal angles of the magnetization in a spherical coordinate system where the poles are perpendicular to the (110) disk plane and the origin of the angle φ is along the [100] axis. The experimental setup sets $\theta = 90°$ in all the performed experiments. The anisotropic energy

$$F = F_Z + F_{dem} + F_{an} \quad (3)$$

is composed of the Zeeman energy F_Z, containing the external field H, the demagnetizing energy F_{dem}, and the magnetocrystalline energy F_{an}. The direction cosines of magnetization for a given magnetic field are found via the expression $\partial F/\partial\varphi \equiv 0$. Equation (2) was used for a least-squares fit to the experimental data of H_{res} in order to obtain the anisotropy constants. The magnetization at different temperatures was partly taken from independent magnetization measurements and the effective
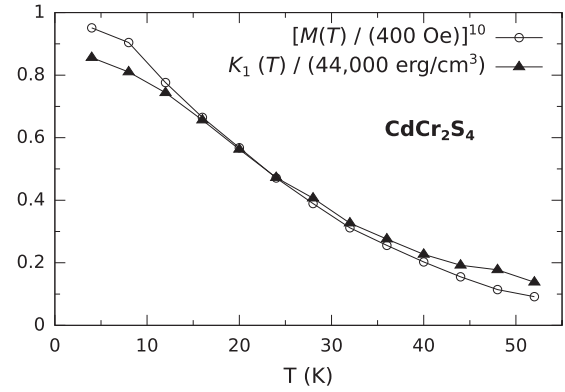

FIG. 6. Comparison of the K_1 values (triangles) normalized to 4.4×10^4 erg/cm^3 with the tenth power of the magnetization values (circles) normalized to 400 Oe.

demagnetizing coefficient of each sample was determined as a fit parameter at one temperature and kept fixed for all other temperatures. The Landé g factor was set to 1.985. For $T \geqslant 20$ K the model of cubic anisotropy fits well to the data, very similarly to the solid lines shown in Fig. 2(a). However, for lower temperatures, not the same quality is reached, mainly because the experimental maxima in the $\langle 111\rangle$ directions are too pronounced, as reported in the literature.[12] This implies that for this system the model of cubic anisotropy is not strictly valid in the whole ferromagnetic temperature range. Omitting anisotropy constants of higher order, we get, nevertheless, $K_1 \approx 4 \times 10^4$ erg/cm^3 at 4 K. The evaluation of the data of H_{res} in the main directions only and under the "K_1-only" assumption yields a reasonable agreement with the tenth-power law[29]

$$\frac{K_1(T)}{K_1(0)} = \left[\frac{M(T)}{M(0)}\right]^{10}, \quad (4)$$

which is characteristic of cubic anisotropy. Deviations in Fig. 6 are notably visible for the low temperatures where the assumption of K_1-only cubic anisotropy seems too simple. Concerning the angular-dependent resonance fields, cubic anisotropy yields good results for the VA sample at temperatures above 40 K (where $K_1 \approx 8 \times 10^4$ erg/cm^3) and for the SA sample down to lowest temperatures, with K_1 reaching the same order as before the treatment. In Fig. 5 it becomes clear that for the SA sample the angular dependence of the resonance field is well described by cubic anisotropy even at low temperatures and no longer is anomalous in the $\langle 111\rangle$ directions.

The peaks of the linewidth in certain directions suggest that a superposition of different anisotropic FMR signals may be a better description for the observations. With a trigonal crystal field resulting in a zero-field splitting of the magnetic ions, it seems likely that the system should be treated as being composed of four uniaxial anisotropy contributions

$$F_{an}^{(i)} = K_{1i}^u\sin^2\beta_i + K_{2i}^u\sin^4\beta_i + K_{3i}^u\sin^6\beta_i + \cdots, \quad (5)$$

where the i represents one of the four Cr^{3+} sites, the β_i is the corresponding direction cosine along the axis of uniaxial anisotropy, i.e., one of the cubic space diagonals $\langle 111\rangle$, and the K_{ni}^u denote the uniaxial anisotropy constants. In this way,

four resonance fields are computed according to Eq. (2). In an ideal case, exchange narrowing combines them to one single resonance observed experimentally:

$$H_{\text{res}} = \langle H_{\text{res}}^{(p)} \rangle = \frac{1}{4} \sum_{p=1}^{4} H_{\text{res}}^{(p)}. \qquad (6)$$

The linewidth is then determined by the second moment M_2 of the resonance fields and is, in a rough approximation, given by[30]

$$\Delta H \cong g\mu_{\text{B}} \frac{M_2}{J} = \frac{g\mu_{\text{B}}}{J} \sum_{p=1}^{4} \left(H_{\text{res}}^{(p)} - \langle H_{\text{res}}^{(p)} \rangle \right)^2, \qquad (7)$$

where J denotes the exchange coupling constant and μ_{B} is Bohr's magneton. Assuming the three anisotropy constants of different orders n to be independent of the atomic site i, the least-squares fit to the resonance field data of the as-grown CdCr$_2$S$_4$ single crystals depicted as the lines in Fig. 2(a) is obtained. Keeping the same fit parameters K_n^{u}, we get, according to Eq. (7), a linewidth simulation which is presented as lines in Fig. 2(b). Obviously, the theoretical model predicts linewidth peaks on the same positions as the experimentally observed anomalies. The constant of proportionality in Eq. (7) was scaled such that observed and computed peaks get the same height at 4 K. From this the estimation $J/k_{\text{B}} = 2.9$ K is obtained, which is only in rough agreement with the value $J/k_{\text{B}} = 11.8$ K, determined from the Curie-Weiss temperature. This deviation seems, however, to be justified, as the expression (7) has been derived for exchange-narrowed paramagnetic electron spin resonance (ESR) lines. The value of $g\mu_{\text{B}}/J$ is then kept constant for all temperatures. Concerning the width of the linewidth peaks and their temperature-dependent height, the result of this calculation yields a good agreement between experiment and theory.

From comparison of the linewidth data in Figs. 3–5 we may conclude that the crystal structure is almost ideal in the as-grown samples, because both annealing processes result in broader FMR lines. Usually these treatments are performed in order to reduce the number of crystal imperfections, whereas on our samples the diffusion processes create considerably more defects, enhancing the overall FMR relaxation. The results for the SA sample help, however, to clarify whether the presence of chromium ions other than Cr^{3+}, caused by nonstoichiometry, can be held responsible for the observed anisotropy. It has to be assumed that Cr^{2+} ions are no longer present after the oxidation reaction and the still existing anisotropy suggests that the distorted CrS$_6$ octahedra are the main cause of it.

The small and slightly anisotropic linewidth maximum at ~ 50 K (Fig. 3) may be an indication of a temperature-peak process[31] arising from a very small amount of paramagnetic impurity atoms. These could, most consistently with the absence of foreign element contaminations, represent Cr^{2+} or Cr^{4+}, thus leading to a valence-exchange relaxation mechanism. In this case from the peak height and from a zero-field splitting parameter $D \approx 0.1$ cm^{-1} typical for Cr^{3+} in a trigonal crystal field,[14] we estimate[32] a foreign valence concentration in the order of 10^{-3}. However, another sample of the same batch with equal anisotropy did not show this feature, which

would rule out a substantial influence of divalent chromium on the anisotropy. Measurements at other microwave frequencies and doping experiments might give a clearer insight into the phenomenon of temperature-peak processes. Generally, we suppose that FMR is even more sensitive to impurities than the x-ray fuorescence described in Sec. II.

V. CONCLUSION

This work was motivated by early reports on the multiferroicity in CdCr$_2$S$_4$ documenting that the dielectric anomalies and the spontaneous polarization as reported in Ref. 6 sensitively depend on synthesis routes and also on possible defect states.[8,18,33]

In the present work we were able to rule out any extrinsic effect which would explain the magnetocrystalline anisotropy in general, and more specifically, its anomalous behavior. We found the occurrence of strong anisotropies along the $\langle 111 \rangle$ directions below 20 K. Our proposed model with local trigonal distortions along the four cube axes works well for temperatures above 20 K and still gives a satisfactory approximation of the data at lowest temperatures. At the same time, the purely cubic description of the data above 20 K is in line with the validity of the tenth-power law between magnetization and anisotropy field. For lower temperatures, the extension to four uniaxial anisotropies coalescing into one ESR line by exchange narrowing helps one to understand the linewidth anomalies. From a theoretical point of view, we assumed that only a trigonal distortion of the CrS$_6$ octahedra (along the four $\langle 111 \rangle$ directions) can partially lift the degeneracy of the spin quartet into two doublets and thus give rise to a locally uniaxial anisotropy.

These local distortions may play a decisive role in the formation of relaxor ferroelectricity. In this respect it is important to be reminded of the old debate about a noncentrosymmetric polar ground state in spinel compounds[34] where it was argued that the off-center ions are experimentally evidenced by unusual large Debye-Waller factors.[35] This debate has brought up a number of questions which remain to be answered.[36] In this context the unexplained contribution to the specific heat[11] may be considered as being correlated to the polar ground state.

Grimes suggested an off-center shift of the B cations along the $\langle 111 \rangle$ directions, resulting in an antiferroelectric ground state. Such a displacement would also yield a uniaxial anisotropy at each of the B sites giving rise to the sharp anomalies in FMR for the field applied along these directions. Smallest amounts of impurities, defects, or even local strain fields will disturb this symmetry-adapted balance of antiferroelectric distortions resulting in local ferroelectric polarization possibly within extended clusters. The formation of polar clusters naturally also would explain the relaxor ferroelectric state detected in CdCr$_2$S$_4$.[6]

[1] T. Rudolf, Ch. Kant, F. Mayr, J. Hemberger, V. Tsurkan, and A. Loidl, New J. Phys. **9**, 76 (2007).

[2] A. N. Yaresko, Phys. Rev. B **77**, 115106 (2008).

[3] V. Tsurkan, H.-A. Krug von Nidda, A. Krimmel, P. Lunkenheimer, J. Hemberger, T. Rudolf, and A. Loidl, Phys. Status Solidi A **206**, 1082 (2009).

[4] R. Moessner and J. T. Chalker, Phys. Rev. Lett. **80**, 2929 (1998).

[5] P. K. Baltzer, P. J. Wojtowicz, M. Robbins, and E. Lopatin, Phys. Rev. **151**, 367 (1966).

[6] J. Hemberger, P. Lunkenheimer, R. Fichtl, H.-A. Krug von Nidda, V. Tsurkan, and A. Loidl, Nature (London) **434**, 364 (2005).

[7] S. Weber, P. Lunkenheimer, R. Fichtl, J. Hemberger, V. Tsurkan, and A. Loidl, Phys. Rev. Lett. **96**, 157202 (2006).

[8] J. Hemberger, P. Lunkenheimer, R. Fichtl, S. Weber, V. Tsurkan, and A. Loidl, Physica B **378-380**, 363 (2006).

[9] G. Harbeke and H. Pinch, Phys. Rev. Lett. **17**, 1090 (1966).

[10] H. Göbel, J. Magn. Magn. Mater. **3**, 143 (1976).

[11] M. Tachibana, N. Taira, and H. Kawaji, Solid State Commun. **151**, 1776 (2011).

[12] S. B. Berger and H. L. Pinch, J. Appl. Phys. **38**, 949 (1967).

[13] H. L. Pinch and S. B. Berger, J. Phys. Chem. Solids **29**, 2091 (1968).

[14] A. Abragam and B. Bleaney, *Electron Paramagnetic Resonance of Transition Ions* (Clarendon Press, Oxford, 1970).

[15] B. Hoekstra, R. P. van Stapele, and A. B. Voermans, Phys. Rev. B **6**, 2762 (1972).

[16] B. Hoekstra and R. P. van Stapele, Phys. Status Solidi B **55**, 607 (1973).

[17] B. Hoekstra, Phys. Status Solidi B **63**, K7 (1974).

[18] S. Krohns, F. Schrettle, P. Lunkenheimer, V. Tsurkan, and A. Loidl, Physica B **403**, 4224 (2008).

[19] Th. Hehenkamp, in *Element-Mikroanalyse zur Qualitätssicherung fester Stoffe* (Christian-Albrechts-Universität zu Kiel, Kiel, 1995).

[20] V. Gnezdilov, P. Lemmens, Yu. G. Pashkevich, Ch. Payen, K. Y. Choi, J. Hemberger, A. Loidl, and V. Tsurkan, Phys. Rev. B **84**, 045106 (2011).

[21] L. R. Walker, J. Appl. Phys. **29**, 318 (1958).

[22] M. Sparks, R. Loudon, and Ch. Kittel, Phys. Rev. **122**, 791 (1961).

[23] J. Kötzler and H. von Philipsborn, Phys. Rev. Lett. **40**, 790 (1978).

[24] J. Kötzler and W. Scheithe, J. Magn. Magn. Mater. **9**, 4 (1978).

[25] J. Kötzler, Phys. Rev. B **38**, 12027 (1988).

[26] M. Hemmida, *Electron Spin Resonance in Frustrated Two- and Three-Dimensional Chromium Magnets* (Dr. Hut, München, 2012).

[27] D. L. Huber, G. Alejandro, A. Caneiro, M. T. Causa, F. Prado, M. Tovar, and S. B. Oseroff, Phys. Rev. B **60**, 12155 (1999).

[28] G. V. Skrotskii and L. V. Kurbatov, in *Ferromagnetic Resonance*, edited by S. V. Vonsovskii (Pergamon Press, Oxford, 1965).

[29] H. B. Callen and E. Callen, J. Phys. Chem. Solids **27**, 1271 (1966).

[30] P. W. Anderson and P. R. Weiss, Rev. Mod. Phys. **25**, 269 (1953).

[31] M. Sparks, *Ferromagnetic Relaxation Theory* (McGraw-Hill, New York, San Francisco, 1964).

[32] Using Eq. (6.6) in Ref. 31.

[33] J. Hemberger, P. Lunkenheimer, R. Fichtl, S. Weber, V. Tsurkan, and A. Loidl, Phase Trans. **79**, 1065 (2006).

[34] N. W. Grimes, J. Phys. C **6**, L78 (1973).

[35] N. W. Grimes, Philos. Mag. **26**, 1217 (1972).

[36] H. Schmidt and E. Ascher, J. Phys. C **7**, 2697 (1974).